Three-way Subsynchronous Torsional Interactions Between LCC HVDC, MMC HVDC and a Thermal Generator

Stefan Kovacevic, *Member*, *IEEE*, Dragan Jovcic, *Fellow*, *IEEE*, Pierre Rault, and Olivier Despouys, *Member*, *IEEE*

***Abstract*—This paper performs a study on three-way subsynchronous torsional interactions (SSTI) between a hybrid dual-infeed high-voltage direct current (HVDC) system and a nuclear generator. The test case is based on the French IFA2000 line commutated converter (LCC) HVDC (2 GW) and the new Eleclink modular multilevel converter (MMC) HVDC (1 GW) interacting with the Gravelines generator (1 GW). The analysis is performed by the means of the eigenvalue stability assessment on an analytical model, while the accuracy of the conclusions is verified using the detailed non-linear electromegnetic transient program (EMTP) model. The study shows that the dual-infeed system may introduce higher risk of the SSTI compared with the point-to-point HVDC systems. It shows that MMC operating as static synchronous compensator (STATCOM) may further reduce the torsional damping at 6.3 Hz mode. This conclusion may be unexpected since it is known fact from literature that STATCOM has a beneficial impact on the transient performance of LCC. Further studies show that in a sequential HVDC loading, it may be beneficial to load the MMC HVDC first. Also, the risk of the SSTI may be minimized by changing HVDC controller gains, in particular, by increasing phase-locked-loop (PLL) gains on the LCC rectifier.**

***Index Terms*—Subsynchronous torsional interaction (SSTI), eigenvalue stability, hybrid dual-infeed high-voltage direct current (HVDC), line commutated converter (LCC), modular multilevel converter (MMC), nuclear generator.**

I. Introduction

THE phenomenon of subsynchronous resonance (SSR) has been manifested in practice on multiple occasions since the 1970s [1], [2]. It represents a condition where the electric network reduces the damping or destabilizes the natural (torsional) modes of a turbine-generator mechanical shaft, which are in the subsynchronous frequency range, i.e., below 50 Hz or 60 Hz [1]. It is manifested with either poorly damped or growing (destabilized) rotor speed oscillations, which may reduce the life-time of the shaft, or even damage the shaft.

The SSR is often associated with series compensated transmission systems; however, it can also be caused by the control of high-voltage direct current (HVDC) transmission, and this is commonly known as the subsynchronous torsional interactions (SSTI) [3]. Reference [4] is the first demonstration of the SSTI, which shows that the line commutated converter (LCC) may destabilize the torsional modes of a nearby turbine-generator at the Square Butte in North Dakota, USA, in 1977. Since then, there have been multiple SSTI cases reported worldwide, even in recent years [5]-[7], and this topic has been well studied [3], [4], [8].

However, there is limited practical experience or published work with the voltage source converter (VSC)-based systems, although this topic is gaining much interest since the emerging VSC topology is superseding the LCC in HVDC applications. Most SSTI studies consider the early two-level VSC and suggest a minor risk [9], [10]. However, modular multilevel converter (MMC) is becoming predominant and has different dynamics from LCC and 2-level VSC [11]. The recent analytical study in [12] shows that an MMC HVDC may significantly reduce the torsional damping of a nearby nuclear generator, and may even cause torsional instability for some realistic operating conditions. However, it is accepted that the impact is generally less adverse compared with LCC HVDC, for the same short circuit capacity (SCC).

With the benefits of MMC, and considering many existing LCC HVDC, we expect to see a mix of MMC and LCC (hybrid dual-infeed HVDC system) interconnecting the same AC grids. This topic is of further interest since studies have indicated that MMC, in either HVDC transmission link or static synchronous compensator (STATCOM) application, may have a beneficial impact on the stability and performance of the LCC [13], [14]. However, previous studies have not examined three-way LCC-MMC-generator torsional interactions, while grid operators are raising new SSTI concerns caused by the combined effect of the two HVDC links.

The aim of this study is to perform three-way SSTI investigation by considering all operating modes. The eigenvalue stability study will be based on a small-signal analytical

Manuscript received: February 23, 2022; revised: May 5, 2022; accepted: July 7, 2022. Date of CrossCheck: July 7, 2022. Date of online publication: August 17, 2022.

This work was supported by Réseau de Transport d'Électricité of France.

This article is distributed under the terms of the Creative Commons Attribution 4.0 International License (http://creativecommons.org/licenses/by/4.0/).

S. Kovacevic and D. Jovcic (corresponding author) are with the School of Engineering, University of Aberdeen, Aberdeen AB24 3UE, U.K. (e-mail: kovac.blok38@gmail.com; d.jovcic@abdn.ac.uk).

P. Rault and O. Despouys are with Réseau de Transport d'Électricité, Paris, France (e-mail: pierre.rault@rte-france.com; olivier.despouys@rte-france.com).

DOI: 10.35833/MPCE.2022.000100

model, which is the best approach for generic, in-depth stability and control design study [1], [11], [15]. The practical test system is presented in Section II, while the EMTP and small-signal state-space models are presented in Section III and IV, respectively. The SSTI stability margins will be evaluated using root locus of the generator torsional modes (eigenvalues) when changing key parameters, operating conditions, and controller gains, which will be presented in Sections V-VII. The results will be verified with detailed simulations on electromegnetic transient program (EMTP) models, which will be given in Section VIII. Finally, conclusions are given in Section IX.

II. Practical Test System

The study is motivated by a practical dual-infeed hybrid HVDC system in the North of France, operated by Réseau de Transport d' Électricité (RTE), the French transmission system operator (TSO). This system has a history of SSTI stability issues [7].

A. North French Topology

The schematic of the test system representing North French topology is presented in Fig. 1. It is composed of an old 2 GW LCC HVDC link IFA2000 (commissioned in 1977 and refurbished in 2012), and the new 1 GW MMC HVDC link Eleclink (2021). The two links connect the French and the English AC grid, and they are of a similar length (70 km). They are connected to the French AC grid within close proximity (10-40 km), as represented by a short tie-line. Although the electrical distance between the links may vary depending on which AC transmission lines are energized, the worst-case closest proximity is considered in the study as guided by the studies with single HVDC links. The two HVDC links are also connected close to the 1.12 GW French nuclear power plant in Gravelines. On the English AC side, each HVDC link is connected to a separate AC grid, since the English terminals are much more distanced. All the HVDC power flow directions are considered, and this covers both the rectifier and the inverter operations on each of the two French converters. Figure 1 also shows two switches (S_1 and S_2), which represent different operating conditions; PCC represents the point of common coupling; X/R is the impedance ratio; and V_{dc} and I_{dc} are the DC voltage and current, respectively.

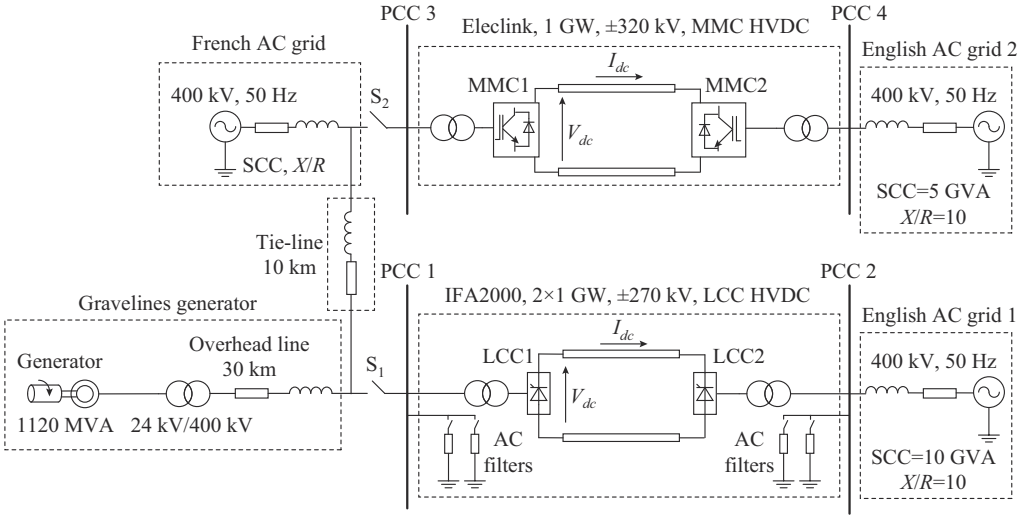

Fig. 1. Schematic of test system representing North French topology.

B. History of SSTI Concerns

In 1988, the Électricité de France (EDF) study reported that the IFA2000 link may destabilize the dominant torsional mode (6.3 Hz) of Gravelines generator, for weak French AC grid [7]. These experimental results were replicated in our recent study with the analytical models [8], confirming the fidelity of the state-space model. Further studies [12] indicated that there may also exist a risk of SSTI with the Eleclink HVDC system. There is now sufficient uncertainty to initiate full and detailed three-way SSTI study.

III. EMTP Model

A. Detailed EMTP HVDC Models

The generator and the LCC HVDC models are represented using the standard electromagnetic transient (EMT) models which are based on the well-documented approaches [16], [17]. The LCC HVDC model is based on the standard 6-pulse converter. The DC cable is represented using the constant distributed-parameter model.

The MMC HVDC is represented using the type 4 average value model according to the CIGRE working group B4.57 [18]. The entire string of cells in one arm is replaced by an equivalent controllable voltage source (schematic available in [11]), and this significantly improves the computational speed. Higher harmonics caused by cell switching and cell voltage variations are neglected since they are out of the interest frequency range. The Eleclink DC cable is represented using the wideband (frequency-dependent) model, as shown in [19].

B. HVDC and Generator Parameters

The parameters of the LCC HVDC are taken from the available IFA2000 data [20] and the industrial experience with similar systems, as presented in [8]. The model includes 8 filters on each AC side, which are switched depending on the HVDC power level. The MMC HVDC parameters are available in [12], and Appendix A gives all key HVDC and generator parameters.

The electrical parameters of Gravelines generator are available in [21]. The generator shaft parameters have been identified in [8] based on oscillatory modes reported by EDF in [7], and are shown in Table I. The analytical model represents well both frequency and damping of the generator torsional modes, i.e., 6.3 Hz, 12 Hz, and 16 Hz mode. The 6.3 Hz mode is the dominant mode (with the lowest damping) while the 16 Hz mode is not excited by the electric network resonance.

TABLE I
GENERATOR SHAFT PARAMETERS

Turbine/generator	Inertia (MWs/MVA)	Spring constant (p.u./rad)	Mechanical damping
High-pressure (HP) turbine	0.168	9.48	0.2
Low-pressure (LP) turbine A	1.390	10.94	0.4
LP turbine B	1.500	19.09	2.0
Generator	0.981		0.4

C. Control Structure

1) LCC HVDC

The LCC HVDC has the standard control structure [11]; each converter has three controllers: DC current, DC voltage, and Gamma extinction angle controllers. In normal operation, the rectifier is controlling DC current and inverter is controlling DC voltage. The converter is synchronized with the PCC voltage using a *dq*-type phase-locked-loop (PLL). During large-signal transients such as AC faults, the DC current controller employs the voltage-dependent-current-order limiter based on the common V_{dc}-I_{dc} graphs. Also, the DC current and DC voltage controllers have proportional gain scheduling [11] with respect to the nominal firing angle (20°).

2) MMC HVDC

The MMC HVDC has the standard control structure [11], which is shown in Fig. 2. Variables are defined in [11]. Rectifier controls active power and inverter controls DC voltage. Each MMC also controls reactive power with AC voltage droop to be compliant with the grid code. As part of the AC voltage primary control, the voltage droop parameter and the voltage reference are defined by the TSO to share the AC voltage control burden between different plants in the same AC area. The outer loop controllers set the reference for the inner decoupled DQ current controller. All controllers operate in the synchronous PCC reference frame using the DQ PLL. Each MMC also employs circulating current suppression controller (CCSC) which is in the double fundamental frequency frame.

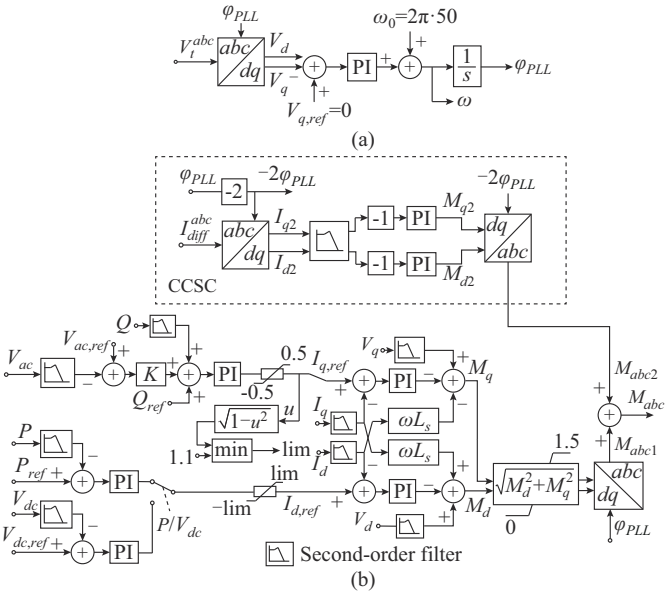

Fig. 2. Schematic of MMC control structure. (a) PLL. (b) Main control.

3) Generator

The generator has generic nuclear generator controllers: the AC4A exciter, the PSS2A power system stabilizer [1], and the IEEEG1 speed governor with load controller [22]. The power system stabilizer has rotor speed and electrical power as the inputs, which has negligible impact on the torsional damping while improving damping of the power swing mode. The load controller is used for slow adjustments of the operating point. Controller details can be found in [8] and [12].

D. Range of HVDC and Generator Controller Gains

The generator controller gains are adopted by considering IEEE standards [22], [23] and they are tuned and tested to provide fast performance with a small overshoot of below 20% for various operating conditions, as shown in [8], [12].

While the generator controller gains are fixed, this study will consider the impact of a wide range of possible HVDC controller gains. The adopted ranges of LCC and MCC HVDC controller gains are provided in Table II and Table III based on RTE field experience, respectively. All the gain values from the given range have been tested and give satisfactory performance.

TABLE II
RANGE OF LCC HVDC CONTROLLER GAINS

Controller	Controller gain	Basic value	Range	Feedback filter
DC current controller	K_P (°/p.u.)	45	±50%	Time constant T_f= 0.0012 s
	K_I (°/(s/p.u.))	4000	±50%	
DC voltage controller	K_P (°/p.u.)	35	±50%	T_f= 0.015 s
	K_I (°/(s/p.u.))	2250	±50%	
Gamma controller	K_P (°/°)	1		
	K_I (°/(°s))	20		
PLL	K_P (rad/(s/p.u.))	10	10-60	
	K_I (rad/(s^2/p.u.))	50	K_P^2/2	

TABLE III
RANGE OF MMC HVDC CONTROLLER GAINS

Controller	Controller gain	Basic value	Range	Feedback filter
Active power controller (P)	K_P (p.u./p.u.)	0		Cut-off frequency f_c = 280 Hz
	K_I (s^{-1}/p.u.)	30	15-45	
Reactive power controller (Q)	K_P (p.u./p.u.)	0		f_c = 280 Hz
	K_I (s^{-1})	30	15-45	
AC voltage droop controller	K (p.u./p.u.)	–6	–9–-3	f_c = 0.5 Hz
	$V_{ac,ref}$ (p.u.)	1		
DC voltage controller (V_{dc})	K_P (p.u./p.u.)	9.6		f_c = 141 Hz
	K_I (s^{-1})	294		
DQ current controller (I_{dq})	K_P (p.u./p.u.)	1		f_{cv} = 11 Hz
	K_I (s^{-1})	100	50-150	f_{cc} = 2000 Hz
PLL	K_P (rad/(s/p.u.))	80	40-120	
	K_I (rad/(s^2/p.u.))	1600	$K_P^2/4$	
CCSC	K_P (p.u./p.u.)	0.8		f_c = 2000 Hz
	K_I (s^{-1})	20		

E. HVDC Operating Strategies

This study assumes that the operating strategy of dual-infeed HVDC system considers the most relevant, as shown in Table IV. The two HVDC links deliver power in the same direction, and both power flow directions are evaluated. Only after one HVDC link is loaded to its rated power can the dispatching of the second link begin, which is termed "sequential" HVDC loading. Either LCC or MMC can be loaded first. In case the MMC is loaded first (operating strategy 2) up to its full power of 1 GW, the LCC is disconnected (the minimum allowable power for the LCC is 10% of the nominal power). However, in case the LCC is loaded first (operating strategy 1), the MMC is operating as STATCOM, which supports AC voltage with reactive power/AC voltage droop control. MMC operating in STATCOM mode is found to have significant impact on system stability, as analyzed in Section V.

TABLE IV
OPERATING STRATEGIES OF DUAL-INFEED HVDC SYSTEM

Type of operation	Operating strategy	Power flow of two HVDC	Total HVDC loading
Sequential HVDC loading	Operating strategy 1	The same direction	0-2 GW: LCC HVDC + STATCOM
			2-3 GW: LCC at 2 GW + MMC HVDC
	Operating strategy 2	The same direction	0-1 GW: MMC HVDC
			1-3 GW: MMC at 1 GW + LCC HVDC

It is possible to increase loading of two HVDC simultaneously and arbitrarily (and perhaps in the opposite direction); however, these operating strategies are not studied.

F. Operating Conditions

This study will analyze broad range of operating points depending on HVDC active/reactive power and generator active power/AC voltage. The French SCC will be reduced from strong to weak grid, with the lowest realistic SCC of 3 GVA according to the TSO [7] (this has not significantly evolved since the studies were performed during the 1980s). Under all operating conditions, the PCC voltage is within the normal operating range ±5% of the rated 400 kV voltage.

IV. SMALL-SIGNAL STATE-SPACE MODEL

The individual small-signal models of the two HVDC links and the generator are coded in MATLAB, and their accuracy has been individually verified against the EMTP models for wide range of operating conditions and for all variables, but they are not presented in detail for brevity.

A. LCC HVDC Model

The linearized state-space LCC HVDC analytical model employs the modeling approaches from [11] and it is outlined in [8]. The state-space DC cable model consists of 10 series π sections which represent well the dynamics up to 1 kHz [24].

B. MMC HVDC Model

The MMC linearized dynamic model is of the 10^{th} order and in three coordinate frames [25]. The complete MMC HVDC model is of the 126^{th} order and includes 2 MMCs, their control systems, and the DC cable [12]. The DC cable is represented as the 50^{th}-order state-space model using frequency-dependent (wideband) vector fitting, and its accuracy is verified against the EMT model up to 1 kHz [24].

C. Generator Model

The linearized generator model in state-space includes rotor/stator circuit, with the armature, field and damper windings, and multi-mass shaft model. The complete linearized model is of the 42^{nd} order and includes the control system [8].

D. Complete Model

The complete test system is assembled in state-space by connecting the subsystems to enable flexibility in studies. The diagram in Fig. 3 shows the block diagram of complete state-space model, including the interconnections, all the controller inputs, as well as the external (AC grid disturbance) inputs. The order of the complete model is 299.

V. SSTI ANALYSIS WITH MMC STATCOM OPERATION

The impact of the French MMC operation as a STATCOM with AC voltage droop control, as defined in Table III, is analysed firstly. The LCC HVDC is delivering power from France to England, since this mode is known to introduce the highest risk of the SSTI.

A. Impact of STATCOM and LCC HVDC Loading

The torsional damping of 6.3 Hz and 12 Hz modes for change of LCC HVDC loading and the French SCC showing also the impact of MMC STATCOM are shown in Fig. 4. The generator is at the rated loading, which is the condition of the lowest torsional damping [1], as it is known from the studies on the point-to-point HVDC [8], [12].

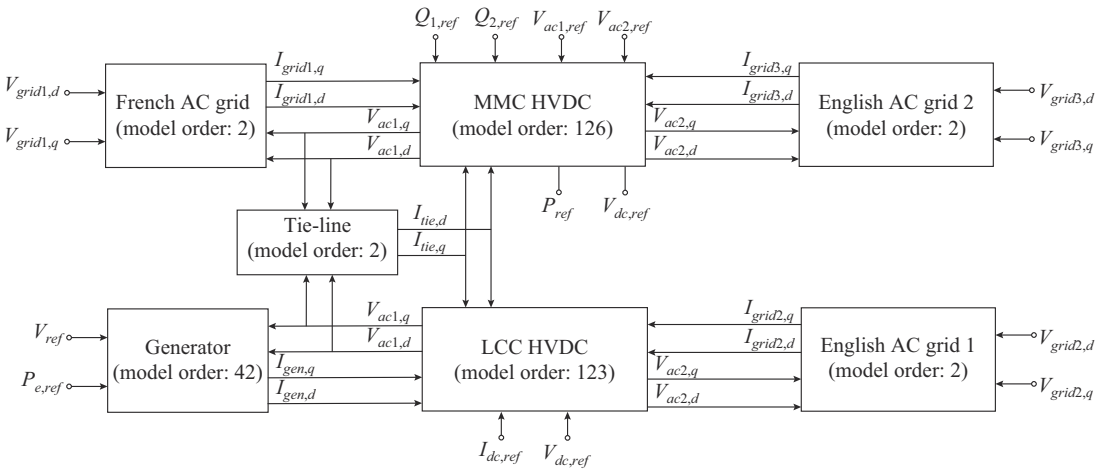

Fig. 3. Block diagram of complete state-space model.

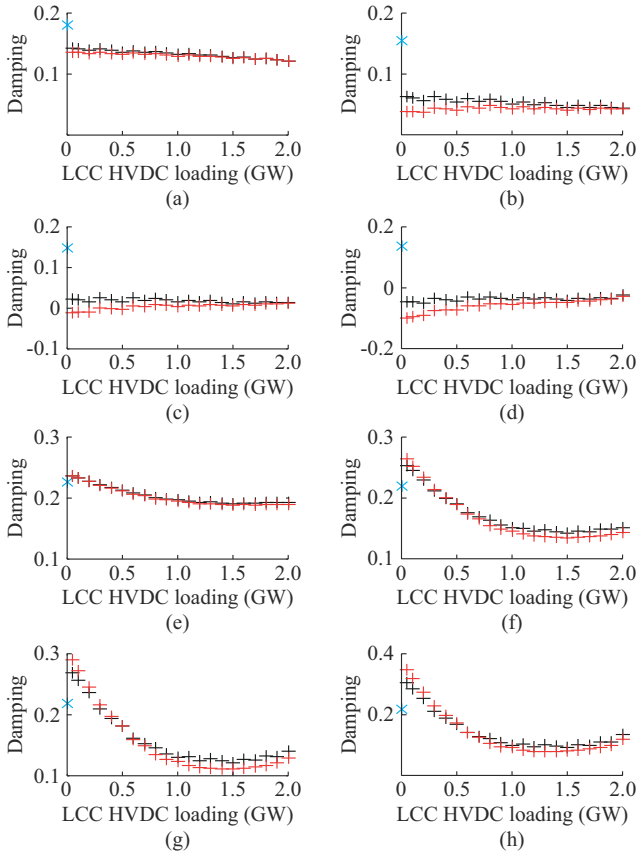

Fig. 4. Torsional damping of 6.3 Hz and 12 Hz modes for change of LCC HVDC loading and French SCC showing also impact of MMC STATCOM. (a) 6.3 Hz mode, French SCC of 10 GVA. (b) 6.3 Hz mode, French SCC of 5 GVA. (c) 6.3 Hz mode, French SCC of 4 GVA. (d) 6.3 Hz mode, French SCC of 3 GVA. (e) 12 Hz mode, French SCC of 10 GVA. (f) 12 Hz mode, French SCC of 5 GVA. (g) 12 Hz mode, French SCC of 4 GVA. (h) 12 Hz mode, French SCC of 3 GVA.

In Fig. 4, the "*" symbol represents the base case of just the generator feeding AC grid (none of the HVDC links is in operation), and it shows that the 6.3 Hz mode always has reduced damping with the HVDC in operation.

Black plots represent the case when only LCC HVDC is connected, which show that LCC always reduces damping across the entire loading range for the 6.3 Hz mode, while the impact on the 12 Hz mode depends on the loading and SCC. Furthermore, the LCC HVDC deteriorates damping more as the French SCC is reducing. For a particularly weak AC grid (SCC below 3.5 GVA roughly), the HVDC may destabilize the 6.3 Hz mode, which is consistent with reports in [7]. The 12 Hz mode is always stable.

The impact of the French MMC operating as STATCOM (zero active power) is shown by red plots. Compared with just LCC HVDC, STATCOM will generally further reduce the damping slightly, although the adverse impact is mostly of significance for lower LCC power. Similar results are obtained for other AC voltages levels in ±5% range, and also for lower generator power, although the torsional damping is higher according to the generator power characteristics [1]. These are unexpected findings, since this STATCOM improves the performance of LCC HVDC (both small signal and transients) when the system is designed using normal voltage stability criteria, as further demonstrated in Section VIII.

B. Impact of STATCOM Controller Settings

Eigenvalue sensitivity of the torsional modes shows that the most influential MMC controller gains are the integral gain of reactive power controller and the droop gain of AC voltage controller. The impact of STATCOM controller gains on the 6.3 Hz mode is shown in Fig. 5 for French SCC of 3 GVA. As can be observed, decreasing these gains reduces negative dynamic impact of the STATCOM but this also degrades the performance of reactive power control (less reactive power contribution or slower reactive power control).

VI. SSTI for Power Flow from France to England

A. Comparison of Strategies for Basic HVDC Controller Gains

Figure 6 shows the torsional damping for the two operating strategies considering change of the French SCC and HVDC loading. In the 0-1 GW range, the operating strategy 2 (MMC HVDC first) has much lower negative impact on the damping, and the torsional modes are not at risk of instability.

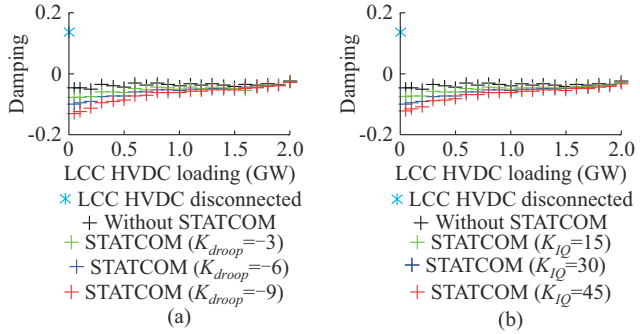

Fig. 5. Impact of STATCOM controller gains on 6.3 Hz mode. (a) K_{droop} = −3, −6, −9. (b) K_{IQ} = 15, 30, 45.

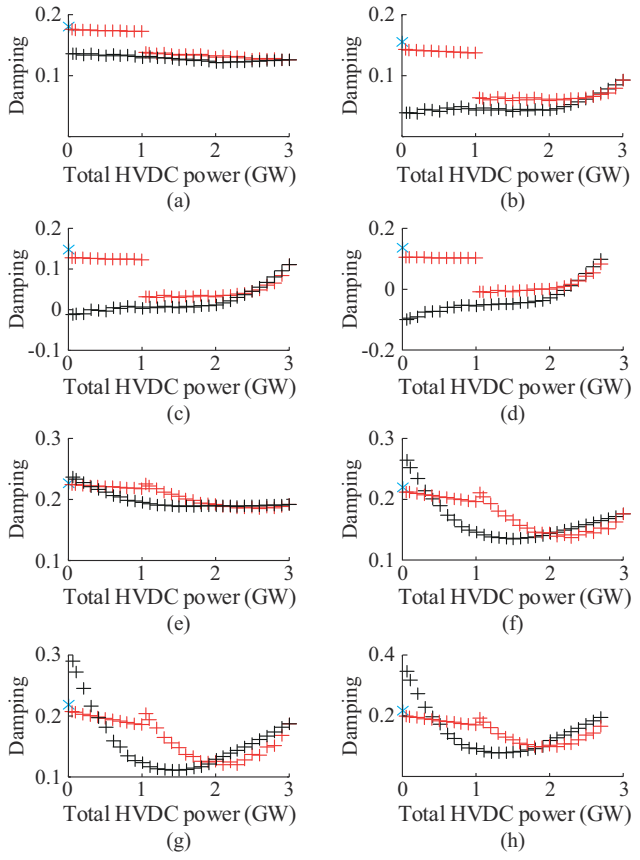

Fig. 6. Torsional damping for two operating strategies considering change of French SCC and HVDC loading. (a) 6.3 Hz mode, French SCC of 10 GVA. (b) 6.3 Hz mode, French SCC of 5 GVA. (c) 6.3 Hz mode, French SCC of 4 GVA. (d) 6.3 Hz mode, French SCC of 3 GVA. (e) 12 Hz mode, French SCC of 10 GVA. (f) 12 Hz mode, French SCC of 5 GVA. (g) 12 Hz mode, French SCC of 4 GVA. (h) 12 Hz mode, French SCC of 3 GVA.

This is expected when comparing previous results for individual HVDC, LCC [8], and MMC [12]. In the 2-3 GW range, the results are similar for the two operating strategies.

However, it is not expected that the damping is improved as the HVDC loading increases, especially in the 2-3 GW range. Further analysis concludes that this is primarily caused by the value of the LCC firing angle. Figure 7 shows that the torsional damping may be very sensitive to the change of the rectifier LCC firing angle, particularly below the nominal value. This is also tested using transformer tap changer on the LCC HVDC, while all other conditions are fixed (similar conclusions are derived in [4]). In the dual-infeed system, Fig. 8 shows that in the 2-3 GW, the PCC voltage decreases since all the AC filters are connected, and MMC has AC voltage droop control. Consequently, the firing angle decreases below the nominal value to maintain the desired power, and this explains why the damping is improving.

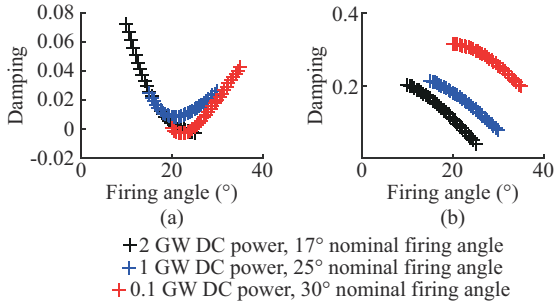

Fig. 7. Torsional damping for change of firing angle. (a) 6.3 Hz mode. (b) 12 Hz mode.

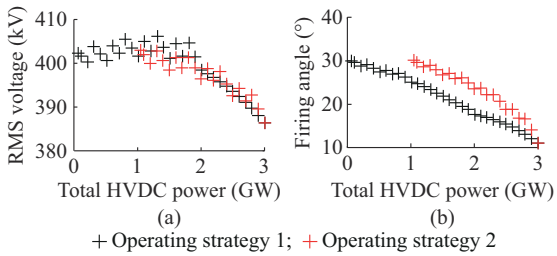

Fig. 8. RMS voltage of PCC and firing angle for change of total HVDC loading. (a) RMS voltage. (b) Firing angle.

B. Impact of HVDC Controller Gains

Eigenvalue sensitivity analysis of the torsional modes is performed on the whole system, and the most influential HVDC controller gains are found to be: DC current controller and PLL gains at the rectifier LCC. This is explored in Fig. 9 for the operating strategy 1, but similar conclusions are derived for the second strategy. In this study, proportional and integral gains are increased simultaneously to maintain similar step performance. It is observed that by increasing the gains at LCC rectifier (either I_{dc} or PLL), the damping of the 6.3 Hz mode is improving significantly, and the risk of destabilizing the mode is eliminated for all the considered operating conditions. This occurs at the expense of some reduction of the damping of the 12 Hz mode. However, this mode has higher inherent mechanical damping and there is no risk of SSTI.

VII. SSTI for Power Flow from England to France

A. Comparison of Strategies for Basic HVDC Controller Gains

Figure 10 presents the torsional damping considering two dual-infeed operating strategies for the case of the French SCC of 7 GVA.

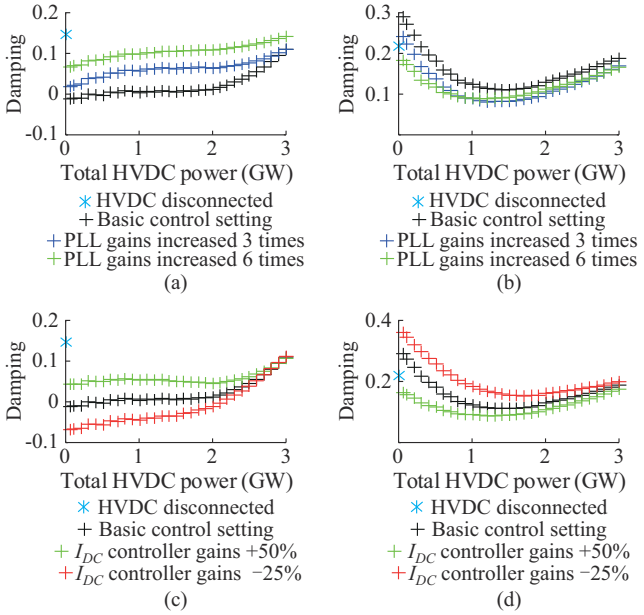

Fig. 9. Torsional damping showing impact of rectifier LCC controller gains. (a) 6.3 Hz mode with different PLL gains. (b) 12 Hz mode with different PLL gains. (c) 6.3 Hz mode with different I_{DC} controller gains. (d) 12 Hz mode with different I_{DC} controller gains.

This is the weakest grid for which the two HVDC links and the generator can deliver full power, according to the power flow analysis. However, similar results are obtained for reduced loading which allows weaker AC grid. The figure shows the damping for the change of the loading of the two HVDC links. Figure 10(a) and (b) shows the impact of the STATCOM operation, while Fig. 10(c) and (d) compares the two operating strategies. As can be observed, the dual-infeed system increases the torsional damping with respect to the isolated generator, and thus, there is no risk of the SSTI.

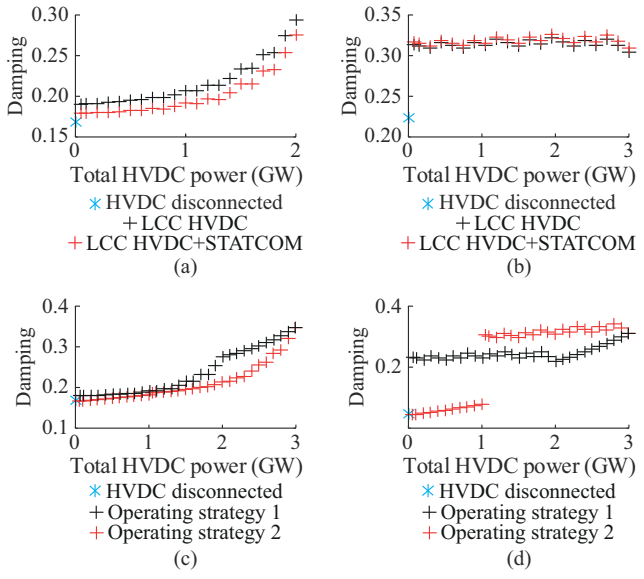

Fig. 10. Torsional damping considering two dual-infeed operating strategies. (a) 6.3 Hz mode with LCC HVDC or STATCOM. (b) 12 Hz mode with LCC HVDC or STATCOM. (c) 6.3 Hz with operating strategy 1 or 2. (d) 12 Hz mode with operating strategy 1 or 2.

B. Impact of HVDC Controller Gains

Additional eigenvalue sensitivity study shows that the dual-infeed system can reduce the torsional damping but of only the 6.3 Hz mode and only when the PLL gains are increased on the inverter LCC. It is shown in Fig. 11 that for high PLL gains (K_P=60, K_I=1800), increasing the total HVDC loading reduces the damping. For high total loading, the 6.3 Hz mode can even become unstable. This conclusion is consistent with other stability studies of interactions between HVDC controllers and weak grids, which concludes that high PLL gains at inverter may cause stability issues [14], [15].

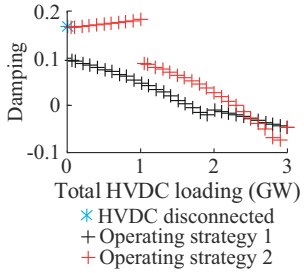

Fig. 11. Damping of the 6.3 Hz mode for high PLL gains at inverter LCC.

VIII. EMT Time Domain Verification

All the results of the eigenvalue study are verified by detailed EMTP simulations. The disturbance (a 2.5% voltage sag) is simulated by connecting a light load (533 MW, 300 Ω resistance) for 0.2 s at the French PCC of the LCC HVDC.

A. Impact of MMC as STATCOM

Literature suggests that STATCOM improves transient performance of LCC HVDC [13], [14], and this is verified in Fig. 12. The responses are obtained for a relatively weak AC grid with SCC of 6 GVA. As can be observed, without STATCOM, LCC HVDC cannot maintain the rated DC current since the rectifier LCC has reached the minimum firing angle of 5°. STATCOM is beneficial since it supports the AC voltage which enables rated power flow. Also, the recovery time, and the damping of the oscillations are improved. Similar conclusions are obtained for all other operating points; however, these studies do not examine the influence of multi-mass generator.

The impact of the STATCOM is now investigated when the generator is operated at rated power and with weak French SCC of 3.5 GVA. Figure 13 shows the obtained generator-rotor speed responses for a voltage sag in 1.5-1.7 s. It can be observed that when the STATCOM is not in operation, the rotor speed has lightly damped oscillations at the frequency of the 6.3 Hz mode.

With STATCOM, the oscillations are similar for the rated LCC power, which means that STATCOM has negligible impact. However, as the LCC power decreases, the impact of STATCOM is to increase the growth rate of the oscillations, which confirms the analytical results obtained in Fig. 4.

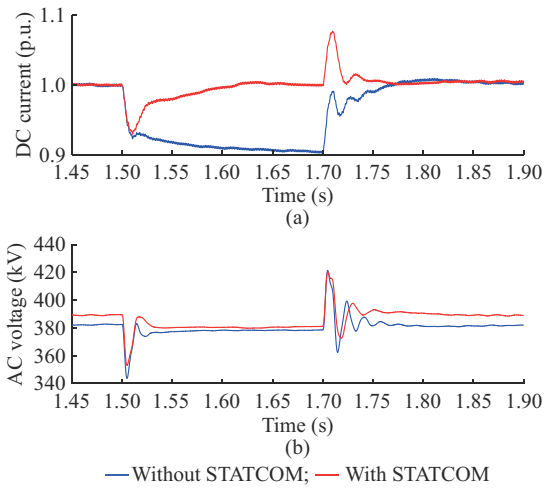

Fig. 12. DC current response on LCC HVDC showing beneficial impact of STATCOM for transient stability. (a) DC current. (b) AC voltage.

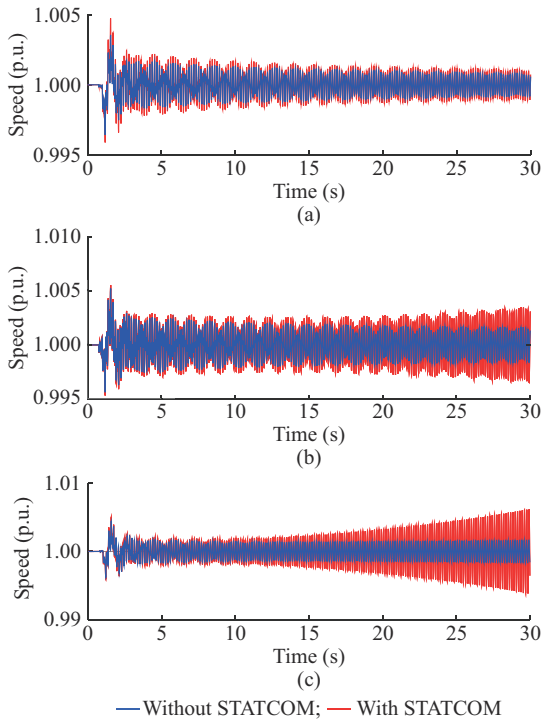

Fig. 13. Generator-rotor speed responses for a voltage sag in 1.5-1.7 s. (a) Rated LCC power. (b) 0.5 p.u. LCC power. (c) 0.1 p.u. LCC power.

B. Hybrid System Consisting of MMC and LCC HVDC Links

The eigenvalue study in Fig. 4 has shown an interesting result that increasing MMC power while LCC HVDC is at rated loading can improve the torsional damping. This is now simulated in EMTP, as shown in Fig. 14. As can be observed, when the MMC is at low power, the generator speed exhibits growing oscillations at the frequency of the 6.3 Hz mode. However, as the MMC power increases, the oscillations become more damped.

C. Impact of PLL Gains

Another important conclusion from analytical study in Fig. 9 is that increasing PLL gains on rectifier LCC can mitigate the SSTI. This is explored on EMTP in Fig. 15, where LCC is operating at rated power with MMC as STATCOM. The French SCC is equal to 3 GVA. As can be observed, for the basic controller gains, the response shows growing oscillations; however, for high PLL gains, the oscillations are well damped and there is no risk of the SSTI. However, on the downside, there is a slight reduction of the 12 Hz oscillation damping.

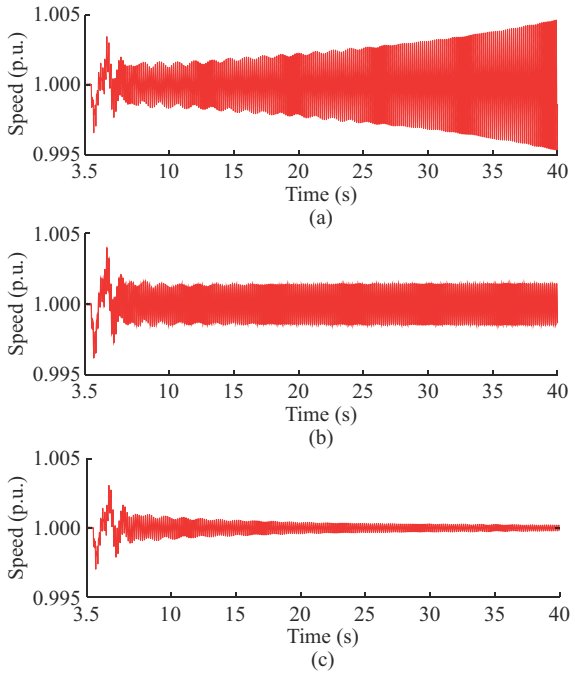

Fig. 14. Generator-rotor speed showing impact of increasing MMC power. (a) MCC HVDC with STATCOM. (b) MCC HVDC with 0.3 GW loading. (c) MCC HVDC with 0.7 GW loading.

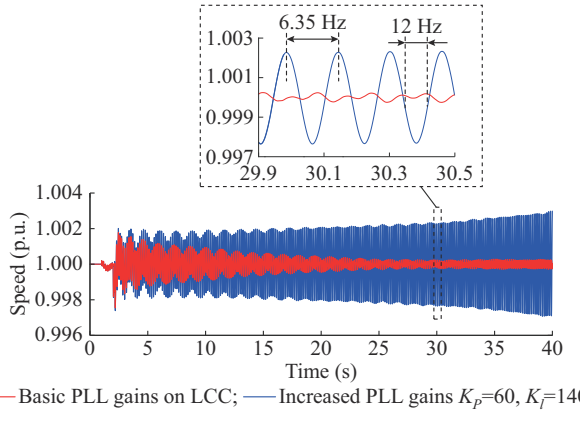

Fig. 15. Generator-rotor speed for a voltage sag.

IX. Conclusion

Three-way LCC-MMC-generator stability analysis has shown that a hybrid dual-infeed HVDC system may introduce a higher risk of the SSTI compared with the individual point-to-point HVDC systems. It is shown that adding an MMC STATCOM may reduce the torsional damping of an existing LCC HVDC and nuclear generator system. In a sequential operation of the dual-infeed system, the risk of the

SSTI may be lower if the MMC HVDC is loaded first. The risk of the SSTI could be mitigated slightly by reducing the STATCOM reactive power or AC voltage droop gains at the expense of voltage control performance. The risk of destabilizing torsional modes may be mitigated by increasing PLL gains on the rectifier LCC. However, increasing PLL gain on the inverter LCC may have an opposite effect on the SSTI.

APPENDIX A

Tables AI-AIII show the LCC HVDC, MMC HVDC, and generator parameters, respectively. Figure A1 shows the parameters of the AC filters on the LCC HVDC.

TABLE AI
LCC HVDC PARAMETERS

Type	Parameter	Value
Converter parameters	HVDC power (GW)	2
	DC voltage rating (kV)	±270
	Smoothing reactance (mH)	350
	Transformer (MVA)	618
	Transformer reactance (p.u.)	0.15
	Transformer ratio (kV)	400/115
DC cable distributed parameters	Resistance (Ω/km)	0.015
	Length (km)	70
	Inductance (mH/km)	0.792
	Capacitance (nF/km)	14.4

TABLE AII
MMC HVDC PARAMETERS

Type	Parameter	Value
Converter parameters	Power rating (MW)	1000
	DC voltage (kV)	±320
	Transformer primary voltage (kV)	400
	Transformer secondary voltage (kV)	360
	Transformer reactance (p.u.)	0.18
	Arm inductance (p.u.)	0.12
	Capacitor energy in submodule (kJ/MVA)	40
	Number of submodules per arm	400
Underground DC cable parameters	Number of poles per cable	2
	Vertical distance from ground level (m)	1.33
	Horizontal distance between poles (m)	0.5
	Conductor outside radius (mm)	32
	Sheath inside radius (mm)	56.9
	Sheath outside radius (mm)	58.2
	Outer insulation radius (mm)	63.9
	Conductor resistivity per length unit (Ω/m)	1.72×10^{-8}
	Sheath resistivity per length unit (Ω/m)	2.83×10^{-8}
	Relative permeability	1
	Insulator relative permittivity	2.5
	Insulator loss factor	0.0004

TABLE AIII
GENERATOR PARAMETERS

Type	Parameter	Value
Basic generator parameters	Power rating (MVA)	1120
	Stator frequency (Hz)	50
	Stator terminal RMS line-to-line voltage (kV)	24
	Number of poles	4
	Armature winding connection (grounded)	Y
Parameters of equivalent electrical circuit	Armature resistance R_a (p.u.)	0.004
	Zero-sequence inductance L_0 (p.u.)	0.187
	Armature leakage inductance L_l (p.u.)	0.27
	Armature d-axis inductance L_d (p.u.)	2.57
	Armature q-axis inductance L_q (p.u.)	2.57
	d-axis transient inductance L'_d (p.u.)	0.411
	d-axis sub-transient inductance L''_d (p.u.)	0.3
	d-axis short-circuit transient time constant T'_d (s)	1.28
	d-axis short-circuit sub-transient time constant T''_d (s)	0.043
	q-axis sub-transient inductance L''_q (p.u.)	0.323
	q-axis short-circuit sub-transient time constant T''_q (p.u.)	0.106

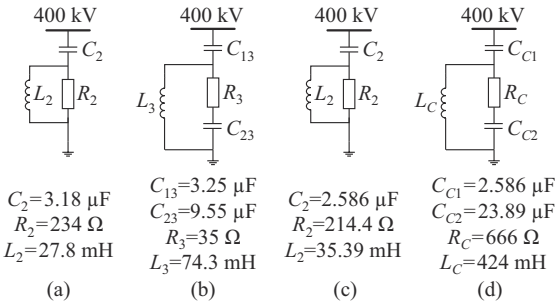

Fig. A1. Parameters of AC filters on LCC HVDC. (a) French side: the 2nd order filter (the 11th and 13th harmonics). (b) French side: the 3rd order filter (the 3rd and 4th harmonics). (c) English side: the 2nd order filter (the 11th harmonic). (d) English side: "C" type filter (the 3rd harmonic).

REFERENCES

[1] P. Kundur, *Power System Stability and Control.* New York: McGraw-Hill, 1994.
[2] P. M. Anderson, B. L. Agrawal, and J. E. V. Ness, *Subsynchronous Resonance in Power Systems*. New York: IEEE Press, 1990.
[3] C. Karawita, "HVDC interaction studies using small signal stability assessment," Ph.D. dissertation, University of Manitoba, Winnipeg, Canada, 2009.
[4] M. Bahrman, E. Larsen, R. Piwko *et al.*, "Experience with HVDC – turbine-generator torsional interaction at Square Butte," *IEEE Transactions on Power Apparatus and Systems*, vol. PAS-99, no. 3, pp. 966-975, May 1980.
[5] Y. Yu, Q. Wei, X. Zhao *et al.*, "Evaluation of subsynchronous oscillation of Xiluodu right station – Guangdong double line ±500 kV DC transmission project," in *Proceedings of 2012 IEEE International Conference on Power System Technology (POWERCON)*, Auckland, New Zealand, Oct.-Nov. 2012, p. 13248588.
[6] W. Du, Z. Zhen, and H. Wang, "The subsynchronous oscillations caused by an LCC HVDC line in a power system under the condition of near strong modal resonance," *IEEE Transactions on Power Delivery*, vol. 34, no. 1, pp. 231-240, Feb. 2019.
[7] P. Bornard, D. Souque, and A. Vieilpeau, "Torsional interactions between the Gravelines units and the 2000 MW cross-channel DC links: protection of the turbine-generator units," in *Proceedings of CIGRE International Conference on Large High Voltage Electric Systems*, Paris, France, Aug.-Sept. 1988, pp. 5-19.
[8] S. Kovacevic, D. Jovcic, O. Despouys *et al.*, "Eigenvalue study of tor-

sional interactions between Gravelines generator and IFA2000 HVDC," in *Proceedings of the 2019 20th International Symposium on Power Electronics*, Novi Sad, Serbia, Oct. 2019, p. 19231985.
[9] N. Prabhu and K. R. Padiyar, "Investigation of subsynchronous resonance with VSC-based HVDC transmission systems," *IEEE Transactions on Power Delivery*, vol. 24, no. 1, pp. 433-440, Jan. 2019.
[10] L. Harnefors, "Analysis of subsynchronous torsional interaction with power electronic converters," *IEEE Transactions on Power Systems*, vol. 22, no. 1, pp. 305-313, Feb. 2007.
[11] D. Jovcic and K. Ahmed, *High Voltage Direct Current Transmission: Converters Systems and DC Grids*, 2nd ed. New York: Wiley, 2019.
[12] S. Kovacevic, D. Jovcic, S. S. Aphale *et al*., "Analysis of potential low frequency resonance between a 1 GW MMC HVDC and a nearby nuclear generator," *Electric Power Systems Research*, vol. 187, p. 106491, Oct. 2020.
[13] C. Guo, W. Liu, C. Zhao *et al*., "Small-signal dynamics and control parameters optimization of hybrid multi-infeed HVDC system," *International Journal of Electrical Power & Energy Systems*, vol. 98, pp. 409-418, Jun. 2018.
[14] S. Kovacevic, D. Jovcic, O. Despouys *et al*., "Comparative stability analysis of LCC, MMC and dual-infeed HVDC operating with weak AC network," in *Proceedings of the 2020 IEEE PES General Meeting (PESGM)*, Montreal, Canada, Aug. 2020, p. 20276873.
[15] D. Jovcic, N. Pahalawaththa, M. Zavahir *et al*., "Small signal analysis of HVDC-HVAC interactions," *IEEE Transactions on Power Delivery*, vol. 14, no. 2, pp. 525-530, Apr. 1999.
[16] H. Dommel, *EMTP Theory Book*. Vancouver: Microtran Power System Analysis Corporation, Apr. 1996.
[17] *IEEE Guide for Synchronous Generator Modeling Practices in Stability Analyses*, IEEE Standard P1110, 2002.
[18] *Guide for the Development of Models for HVDC Converters in a HVDC Grid*, CIGRE Working Group B4.57, 2014.
[19] O. Ramos, L. Naredo, J. Mahseredjian *et al*., "A wideband line/cable model for real-time simulations of power system transients," *IEEE Transactions on Power Delivery*, vol. 27, no. 4, pp. 2211-2218, Oct. 2012.
[20] *Experience Feedback on the Cross-channel 2000 MW Link After 20 Years of Operation*, CIGRE Working Group B4-203, 2006.
[21] P. H. Adam and Z. Yao, "Validation of digital simulation for studies of torsional interaction between a turbo-generator and an HVDC link," in *Proceedings of International Conference on AC and DC Power Transmission*, London, UK, Sept. 1991, p. 4031712.
[22] *Dynamic Models for Turbine – Governors in Power System Studies*, Tech. Rep. PES-TR1, IEEE Power & Energy Society, USA, 2013.
[23] *IEEE Recommended Practice for Excitation System Models for Power System Stability Studies*, IEEE Standard 421.5-2016, 2016.
[24] S. Kovacevic, D. Jovcic, P. Rault *et al*., "Small signal state space model of the frequency-dependent DC cable based on direct vector fitting," in *Proceedings of the 15th IET International Conference on AC and DC Power Transmission*, Coventry, UK, Feb. 2019, pp. 1-6.
[25] A. Jamshidifar and D. Jovcic, "Small signal dynamic DQ model of modular multilevel converter for system studies," *IEEE Transactions on Power Delivery*, vol 31, no. 1, pp. 191-199, Feb. 2016.

Stefan Kovacevic received the M. Sc. degree in power system engineering from the University of Belgrade, Belgrade, Serbia, in 2016, and the Ph. D. degree in electrical engineering from the University of Aberdeen, Aberdeen, U.K., in 2021. Currently, he is working at Jacobs, a consultancy company since 2021, and he has worked as a Research Fellow at the University of Aberdeen in the period 2020-2021. His research interests include HVDC technology, integration of renewable energy into AC and DC grids.

Dragan Jovcic received the Diploma Engineer degree in control engineering from the University of Belgrade, Belgrade, Serbia, in 1993, and the Ph. D. degree in electrical engineering from the University of Auckland, Auckland, New Zealand, in 1999. He is currently a Professor with the University of Aberdeen, Aberdeen, U. K., where he has been since 2004. In 2008, he held Visiting Professor post at McGill University, Montreal, Canada. He also worked as a Lecturer with University of Ulster, Jordanstown, UK, in the period 2000-2004, and as a design Engineer in the New Zealand power industry, Wellington, New Zealand, in the period 1999-2000. His research interests include HVDC, FACTS, and DC grids.

Pierre Rault received the Ph. D. degree in electrical engineering from the École Centrale de Lille, Lille, France, in 2014. He is currently a Senior Engineer for HVDC research and development activities with the Réseau de Transport d' Électricité (RTE) and RTE International, Paris, France. His research interests include HVDC, FACTS, offshore wind farms, interactions between high-voltage power electronic systems, and integration of power electronics into power systems.

Olivier Despouys holds a M. Sc. degree from engineering school ENSEEIHT, Toulouse, France, and a Ph. D. degree. from LAAS-CNRS in Toulouse, France. He worked for Électricité de France (EDF), Paris, France before joining Réseau de Transport d' Électricité (RTE), Paris, France, where he started working in 2009 on specifications for HVDC interconnections, European grid code for HVDC, and research projects related to DC technologies. Regarding EU R&D projects, he was in charge of TWENTIES demo 3 (feasibility of offshore DC grids) and Best Paths demo 2 (interoperability for VSC HVDC). He is currently R&D Project Manager for HVDC and Power Electronics, in charge of a portfolio of research activities at RTE. He is also the Regular Member of CIGRE B4 (DC and power electronics) for France. His research interests include HVDCC and MVDC technologies and grid expansion planning.